Application of renormalization to potential scattering

1997 J. Phys. A: Math. Gen. 30 4687

(http://iopscience.iop.org/0305-4470/30/13/020)

J. Phys. A: Math. Gen. **30** (1997) 4687–4700. Printed in the UK PII: S0305-4470(97)78081-8

Application of renormalization to potential scattering

Carlos F de Araujo Jr†, Lauro Tomio†, Sadhan K Adhikari†§ and T Frederico‡

Instituto de Física Teórica, Universidade Estadual Paulista, 01405-900 São Paulo, São Paulo, Brasil

Departamento de Física, Instituto Tecnológico da Aeronáutica, Centro Técnico Aeroespacial, 12228-900 São José dos Campos, São Paulo, Brasil

Received 23 September 1996, in final form 25 February 1997

Abstract. A recently proposed renormalization scheme can be used to deal with nonrelativistic potential scattering exhibiting ultraviolet divergence in momentum space. A numerical application of this scheme is made in the case of potential scattering with r^{-2} divergence for small r, common in molecular and nuclear physics, by using cut-offs in momentum and configuration spaces. The cut-off is finally removed in terms of a physical observable and model-independent result is obtained at low energies. The expected variation of the off-shell behaviour of the t-matrix arising from the renormalization scheme is also discussed.

1. Introduction

Ultraviolet divergences commonly occur in field theories, as a consequence of point-like interactions in the original Lagrangian, both in perturbative expansions and exact solutions. These divergences in perturbative quantum field theory could be eliminated by renormalization to yield a scale [1, 2] and with few exceptions the renormalized perturbative series could not be summed.

In quantum scattering and bound states calculations, a similar situation occurs for potentials with certain singular behaviour at short distances. In momentum space such problems develop ultraviolet or large momentum divergence. In these cases, both perturbative and exact methods fail to obtain a finite solution.

Motivated by the kind of equations that appear in quantum field theories, the renormalization ideas have been discussed in configuration [3, 4] and momentum [5–8] spaces for potential scattering, where Dirac delta, contact, or zero-range potentials were used. Such potentials have the advantage of being simple, local and separable, with the additional advantage that all discussions can be analytical [5, 7].

Usually, renormalization is carried out by introducing a sufficiently large (small) cut-off in momentum (configuration) space. With this cut-off the divergences of the original problem are avoided and a meaningful result is obtained. In a successful renormalization scheme the knowledge of a physical observable at a particular energy is used to eliminate the cut-off and the final renormalized results should be independent of the detailed renormalization scheme in the limit when the momentum (configuration) cut-off is removed to infinity (zero). Renormalization of these potential models leads to new scales and finite physical observables [5].

§ John Simon Guggenheim Memorial Foundation Fellow.

0305-4470/97/134687+14$19.50

The purpose of this work is to perform numerical renormalization of a quantum mechanical problem where an analytical solution is not possible. In this way, we can study and understand better the on- and off-shell behaviour of the resulting t-matrix, arising from different regularization schemes. We consider renormalization of S-wave potential scattering with a local attractive potential singular at $r \to 0$, given by

$$V(r) = V_0 \frac{\exp(-\mu r)}{r^2}. \tag{1}$$

In addition to performing general numerical renormalization with this potential, we shall be particularly interested in studying the expected off-shell behaviour of different regularization procedures in the nucleon–nucleon interaction. For a sufficiently large $|V_0|$, the scattering problem with potential (1) exhibits ultraviolet divergence and does not permit solutions [9]. At negative energies an infinite number of bound states collapse to infinite binding and at positive energies the scattering equation has a noncompact kernel and does not allow a scattering solution. For a very small $|V_0|$ these theoretical problems can be avoided but the problem becomes difficult to handle numerically.

It is appropriate to mention that, in the limit of $\mu = 0$, the critical strength given in [9] is

$$V_{0,\mathrm{crit}} = -\frac{1}{4}\left(\frac{\hbar^2}{2m}\right) \tag{2}$$

where m is the reduced mass of the two-body system separated by distance r. For attractive (negative) potentials, with $|V_0| > |V_{0,\mathrm{crit}}|$, one encounters an infinite number of bound states with infinite binding. For $|V_0| < |V_{0,\mathrm{crit}}|$, these infinite number of bound states are absent. For a finite nonzero μ, as the short-range divergent behaviour of potential (1) is unchanged, similar properties are expected. This behaviour is apparent in our numerical results.

The motivation behind studying this potential is that similar potentials occur in various branches of physics, such as molecular, nuclear and atomic physics [10]. Also, from a mathematical point of view, renormalization in quantum mechanics is an interesting field. Potential (1) has particular interest in molecular and nuclear physics. The meson-exchange field-theoretic nucleon–nucleon potentials have terms similar to that in equation (1). Potentials with similar behaviour also appear in molecular physics. Such terms are treated phenomenologically by introducing an arbitrary cut-off at small r or large momentum so as to cure the original divergences and to fit some observables. As the problem is mathematically divergent, the results could be very sensitive to the cut-off and it is not clear whether the momentum cut-off can be taken to infinity in order to produce a meaningful renormalization of the problem. In nucleon–nucleon potentials the finite size of the hadrons sets a cut-off in both momentum and configuration spaces, and one should work with a finite cut-off. However, it would be pleasing to see that the results do not get drastically modified as the momentum cut-off is taken to infinity.

In the present work the above problem is renormalized numerically by the introduction of a momentum or configuration space cut-off in different ways. The cut-off is introduced in the Green's function or the potential in momentum and configuration spaces, respectively. The cut-off is finally eliminated in favour of a physical observable/information, which is chosen to be the scattering length and the number of bound states of the system. Eventually, we find that by taking the cut-off to infinity, model-independent results are obtained. An example of this scheme can be found in [11], where the binding energy was used as the physical observable. Though in the nucleon–nucleon system one has utmost a single bound state, there could be several bound states in atomic/molecular systems. In this study we

have used up to four bound states in order to explore the applicability of the renormalization scheme to these general problems.

The regularization of the solution by modifying the Green's function is standard in particle and intermediate energy physics. In atomic, molecular and nuclear physics the traditional method is to modify the potential by form factors. This latter procedure is comparable with the modification of the potential at short distances or large momentum as has been done in this work. We demonstrate an equivalence between both schemes for on-shell scattering.

Although most aspects of the present study are quite general, we shall examine some special aspects of interest to nucleon–nucleon scattering. In addition to the on-shell scattering under diverse situations, we also studied the problem of off-shell scattering with potential (1) with a single bound state in some details as that potential simulates nucleon–nucleon scattering. It is well known that the knowledge of all on- and half-on-shell t-matrix elements is enough to produce the fully off-shell t-matrix elements [12]. This is why we only study the half-shell function [13]. These elements are also interesting from a physical point of view as they are precisely the elements which can be probed experimentally in a Bremsstrahlung experiment [14]. From the present study we determine the extent of the off-shell variation of the phenomenological nucleon–nucleon potentials arising from different regularization schemes.

In this study, in addition to one bound state, we also considered up to four bound states for potential (1). The appearance of few bound states is common in atomic and molecular physics, though in the nucleon–nucleon system commented above there is at most one bound state. The successful renormalization of potential (1) in the presence of several bound states suggests that the present renormalization scheme should be applicable to similar potentials in atomic and molecular physics.

Similar renormalization has been performed recently in quantum mechanics for the one-dimensional x^{-2} potential and the three-dimensional Hulthen potential by Gupta and Rajeev [15], where the interest of such potentials in polymers has been emphasized [16].

The paper is organized as follows. In section 2, we briefly describe the renormalization scheme in quantum mechanics, in the case of a general local potential, following [7]. In section 3 we describe the different regularization procedures applied to the scattering equation for the potential given by equation (1). Finally, in section 4, we present results and main conclusions.

2. Renormalization in quantum mechanics

In operator notation, the Lippmann–Schwinger equation for the t-matrix T is given by

$$T(E) = V + VG_0(E)T(E) \tag{3}$$

where $G_0(E)$ is the free Green's function operator,

$$G_0(E) = (E - H_0 + \mathrm{i}0)^{-1} \tag{4}$$

H_0 is the free Hamiltonian and E is the centre-of-mass energy. V is the potential that, in the present case, is given by equation (1).

The partial-wave projection of a matrix element of the operator $\mathcal{O}$ ($\equiv T$ or V) in momentum space, for a spherically symmetric potential, is given by

$$\langle \boldsymbol{p}|\mathcal{O}|\boldsymbol{q}\rangle \equiv \frac{2}{\pi}\sum_{l=0}^{\infty}\mathcal{O}_l(p,q)\sum_{m=-l}^{l}Y^*_{l,m}(\Omega_p)Y_{l,m}(\Omega_q)$$

$$= \frac{2}{\pi}\sum_{l=0}^{\infty}\mathcal{O}_l(p,q)\frac{2l+1}{4\pi}P_l\left(\frac{\boldsymbol{p}\cdot\boldsymbol{q}}{pq}\right) \tag{5}$$

where $Y_{l,m}(\Omega_p)$ are the usual spherical harmonics normalized to one, Ω_p represents the two polar angles of $\boldsymbol{p}$, and $p = |\boldsymbol{p}|$. $P_l(x)$ is the usual Legendre polynomial of order l and $\mathcal{O}_l(p,q)$ is the coefficient of the expansion.

Using equation (5) in equation (3) for a central potential, after the integrations in the angular variables (where we use the orthonormalization condition of the spherical harmonics), we obtain the corresponding partial wave projection of equation (3):

$$T_l(p,p';E) = V_l(p,p') + \frac{2}{\pi}\int_0^{\infty} q^2\,\mathrm{d}q\; V_l(p,q)G_0(q;k^2)T_l(q,p';E) \tag{6}$$

where $E = k^2$, in units such that $\hbar = 2m = 1$, with m being the reduced mass. The momentum-space free Green's function is given by

$$G_0(q;k^2) = (k^2 - q^2 + \mathrm{i}0)^{-1}. \tag{7}$$

With the definition given in equation (5), applying the Fourier transform of the local potential $V(r)$ to momentum space, we can easily obtain the momentum space partial wave coefficients, as follows. From equation (5), by defining $x \equiv \boldsymbol{p}\cdot\boldsymbol{q}/(pq)$ and applying the usual normalization of the Legendre polynomials, we have

$$\begin{aligned} V_l(p,q) &= \pi^2\int_{-1}^{1}\mathrm{d}x\; P_l(x)\langle\boldsymbol{p}|V|\boldsymbol{q}\rangle \\ &= \pi^2\int_{-1}^{1}\mathrm{d}x\; P_l(x)\frac{1}{(2\pi)^3}\int\mathrm{d}^3r\; V(r)\exp\left(\mathrm{i}(\boldsymbol{p}-\boldsymbol{q})\cdot\boldsymbol{r}\right) \\ &= \frac{1}{2}\int_0^{\infty} r^2\mathrm{d}r\; V(r)\int_{-1}^{1}\mathrm{d}x\; P_l(x)\frac{\sin(|\boldsymbol{p}-\boldsymbol{q}|r)}{|\boldsymbol{p}-\boldsymbol{q}|r}. \end{aligned} \tag{8}$$

Next, we use the addition theorem given in equation (10.1.45) of [17]:

$$\frac{\sin(|\boldsymbol{p}-\boldsymbol{q}|r)}{|\boldsymbol{p}-\boldsymbol{q}|r} = j_0\left(r\sqrt{p^2+q^2-2pqx}\right) = \sum_{n=0}^{\infty}(2n+1)\,j_n(pr)\,j_n(qr)P_n(x) \tag{9}$$

where $j_l(z)$ are spherical Bessel functions of order l (see [17, ch 10]). Finally, using the normalization condition of the Legendre polynomials, we obtain a simplified expression for our definition of the l-wave projection of a matrix element of local potential in momentum space:

$$V_l(p,q) = \int_0^{\infty} r^2\mathrm{d}r\; V(r)\,j_l(pr)\,j_l(qr). \tag{10}$$

As we are going to consider only the S-wave ($l = 0$) case, in the following we simplify the notation by neglecting the l indices.

With the above partial wave projection, the S-wave scattering length a and the off-shell function $f(p,k)$ are defined, respectively, by

$$a = T(0,0;0) \tag{11}$$

and

$$f(p,k) = \frac{T(p,k;k^2)}{T(k,k;k^2)}. \tag{12}$$

In [7], a constant potential in momentum space, $V(p',p) = \lambda$, was chosen to exemplify the application of the renormalization scheme in quantum mechanics. With such potential the

above equation presents ultraviolet divergence, because the kernel of the integral equation is noncompact and equation (6) does not have scattering solution.

So, to give meaning to equation (6), when it presents ultraviolet divergence, a new regularized equation should be defined, where the Green function or the potential is replaced by a regularized one with a cut-off parameter in momentum space (Λ) or configuration space (α), respectively. Such regularization truncates the large-momentum parts of this equation and eliminates the ultraviolet divergence. The cut-off parameter is finally eliminated in terms of a physical observable, in order to yield a renormalized t-matrix which should be independent of the regularization procedure. The Green's function and potential regularizations should lead to equivalent results, when the cut-off is removed by taking the limit $\Lambda \to 0$ or $\alpha \to 0$, respectively. We show in the following that the phase shifts calculated through a Green's function regularization is very similar to those calculated through a potential regularization in the above limit.

One way of introducing a regularized Green's function is to multiply the free Green's function by a regulator function $v(q, \Lambda; k)$ that contains a smooth cut-off $\Lambda(> k)$, such that

$$G_R(q, \Lambda; k^2) \equiv \frac{v^2(q, \Lambda; k^2)}{(k^2 - q^2 + \mathrm{i}0)}. \tag{13}$$

The function $v(q, \Lambda; k)$ satisfies the conditions

$$v(k, \Lambda; k) = 1 \tag{14}$$

and

$$\lim_{\Lambda \to \infty} v(q, \Lambda; k) = 1. \tag{15}$$

For an appropriate $v(q, \Lambda; k)$ the regularized scattering equation,

$$T_R(p, p'; E) = V(p, p') + \frac{2}{\pi} \int_0^\infty q^2 \, \mathrm{d}q \, V(p, q) G_R(q, \Lambda; k^2) T_R(q, p'; E) \tag{16}$$

has no ultraviolet divergence.

In case of a constant potential in momentum space, the following regulator function was introduced in [7]:

$$v^2(q, \Lambda; k) \equiv \frac{(\Lambda^2 + k^2)}{(\Lambda^2 + q^2)}. \tag{17}$$

For other potentials presenting ultraviolet divergence, one can try the same regulator function $v(q, \Lambda; k)$, or, (in case of stronger divergence) replace it by another convenient function.

The regularization procedure used above guarantees unitarity because the imaginary part of the Green's function is unaffected. However, the limit $\Lambda \to \infty$ reduces the regularized Green's function to the free Green's function and the original ultraviolet divergence reappears. The renormalized t-matrix is obtained by eliminating the cut-off Λ in favour of a physical observable at some specific energy.

The above regularization through the Green's function, as given in [7], is on-shell equivalent to a regularization through the potential. To demonstrate this, let us regularize equation (6) using the following regularized potential

$$V_R(p, p') = v(p, \Lambda; k) V(p, p') v(p', \Lambda; k) \tag{18}$$

and keeping the Green's function unchanged.

Now the regularized t-matrix elements satisfy

$$T'_R(p, p'; E) = V_R(p, p') + \frac{2}{\pi} \int_0^\infty q^2 \, \mathrm{d}q \, V_R(p, q) G_0(q; k^2) T'_R(q, p'; E). \tag{19}$$

The on-shell equivalence of both schemes can be shown by the relation between T_R and T'_R, that can be obtained by replacing V_R, in equation (19), by equation (18):

$$\begin{aligned} T'_R(p, p'; E) &= v(p, \Lambda; k) T_R(p, p'; E) v(p', \Lambda; k) \\ &= v(p, \Lambda; k)\Bigg[V(p, p') + \frac{2}{\pi}\int_0^\infty q^2 \, \mathrm{d}q \\ &\quad \times V(p, q)\frac{v^2(q, \Lambda; k)}{(k^2 - q^2 + \mathrm{i}0)} T_R(q, p'; E)\Bigg] v(p', \Lambda; k). \end{aligned} \tag{20}$$

Considering that the function $v(p, \Lambda; k)$ should satisfy equation (14), all the on-shell scattering observables derived by using T_R or T'_R are identical. Differences between the two approaches can only be detected when calculating off-shell observables.

3. Models for regularization and renormalization

Fredholm reduction of the Lippmann–Schwinger equation for the t-matrix has a numerical advantage in dealing with real algebra and one such scheme was used for numerical solution. Auxiliary Fredholm real Γ-matrix equation was solved numerically [18, 19]. The Γ-matrix equation avoids the fixed point singularity and has a much weaker kernel. (For such reduced kernel techniques we refer the reader to [13] and references therein.) When accurate numerical results are needed, the iterative procedure applied to the Γ-matrix integral equation has considerable advantages, compared with the matrix inversion methods, as shown in [19].

In this section we apply the renormalization scheme presented in the previous section to solve the scattering equation with potential (1). For a large enough $|V_0|$, this potential has a singular behaviour at the origin and admits a ground state with infinite energy, which is physically meaningless.

To test numerically the renormalization scheme we apply four regularization procedures for S-wave scattering with this potential. In two of them we have introduced a regulator function in the Green's function as described in the previous section. In the other two approaches we introduce a cut-off directly in the configuration space expression of the potential, so that a simple regulator function in momentum space cannot be factorized. We describe the four schemes (A, B, C, and D) as follows.

Choice A. The S-wave momentum-space representation of potential (1), after solving equation (10) for $l = 0$, with the help of equation (3.947.2) of [20], is given by

$$V(p, q) \equiv \frac{V_0}{2pq}\left[p \arctan\frac{2\mu q}{\mu^2 + p^2 - q^2} + q \arctan\frac{2\mu p}{\mu^2 + q^2 - p^2} + \frac{\mu}{2}\ln\frac{\mu^2 + (p-q)^2}{\mu^2 + (p+q)^2}\right] \tag{21}$$

with the following limiting behaviour

$$V(0, q) = V(q, 0) = \frac{V_0}{q}\arctan\left(\frac{q}{\mu}\right). \tag{22}$$

The regulator function in the Green's function is taken to be the following cut-off step function:

$$v^2(p, \Lambda_A; k) = \Theta(\Lambda_A - p) \tag{23}$$

where $\Theta(x) = 1$ for $x > 0$ and equal to 0 for $x < 0$.

Choice B. The potential $V(p,q)$ is also given by equation (21), but in this case the regulator function in the Green's function is taken to be a smooth cut-off function:

$$v^2(p,\Lambda_B;k) \equiv \frac{(\Lambda_B^2+k^2)}{(\Lambda_B^2+p^2)}. \tag{24}$$

Choice C. The regularization procedure is given in the configuration space, through a cut-off α_C, included in the potential, such that in the limit $\alpha_C \to 0$ the regularized potential reduces to equation (1). In this case the potential used in the calculation is given by

$$V_C(r) = \frac{V_0 \exp(-\mu r)}{r(r+\alpha_C)}. \tag{25}$$

The corresponding S-wave momentum-space matrix element of potential $V_C(p,q)$ is given by

$$\begin{aligned} V_C(p,q) &= \frac{V_0 e^{\mu\alpha_C}}{4pq}\int_\mu^\infty dz\,\exp(-\alpha_C z)\ln\left(\frac{z^2+(p+q)^2}{z^2+(p-q)^2}\right) \\ &= \frac{V_0}{4\alpha_C pq}\ln\left(\frac{\mu^2+(p+q)^2}{\mu^2+(p-q)^2}\right) \\ &\quad -\frac{2V_0}{\alpha_C}e^{\mu\alpha_C}\int_\mu^\infty dz\,\frac{z\exp(-\alpha_C z)}{[z^2+(p+q)^2][z^2+(p-q)^2]} \\ &= \frac{V_0\mu e^{\mu\alpha_C}}{4pq}\int_0^1 dy\,\frac{\exp(-\mu\alpha_C/y)}{y^2}\ln\left(\frac{\mu^2+(p+q)^2y^2}{\mu^2+(p-q)^2y^2}\right) \end{aligned} \tag{26}$$

with the limiting behaviour

$$V_C(p,0) = V_C(0,p) = V_0 e^{\mu\alpha_C}\int_\mu^\infty dz\,\frac{\exp(-\alpha_C z)}{z^2+p^2} = V_0\mu e^{\mu\alpha_C}\int_0^1 dy\,\frac{\exp(-\alpha_C\mu/y)}{\mu^2+(py)^2}. \tag{27}$$

Choice D. The procedure for regularization is given in configuration space, through a cut-off α_D, such that in the limit $\alpha_D \to 0$, V reduces to equation (1). The regularized potential for this choice is

$$V_D(r) = \frac{V_0\exp(-\mu r)}{(r+\alpha_D)^2} \tag{28}$$

and the corresponding S-wave momentum-space potential $V_D(p,q)$ is given by

$$\begin{aligned} V_D(p,q) &= 2V_0 e^{\mu\alpha_D}\int_\mu^\infty dz\,\frac{z(z-\mu)\exp(-\alpha_D z)}{[z^2+(p+q)^2][z^2+(p-q)^2]} \\ &= 2V_0 e^{\mu\alpha_D}\mu^3\int_0^1 dy\,\frac{(1-y)\exp(-\mu\alpha_D/y)}{\mu^4+2\mu^2y^2(p^2+q^2)+(p^2-q^2)^2y^4}. \end{aligned} \tag{29}$$

For choices A and B the regulator function is introduced in the Green function, as explained in section 2. For choices C and D, the cut-off is introduced directly in the configuration space expression of the potential, before the Fourier transform is taken, such that a regulator function cannot be simply factorized in momentum space, as in choices A and B.

The results for the various renormalization schemes is expected to be independent of the detailed regularization procedures. Such an expectation is verified in numerical calculation in the next section, and its limitation is discussed.

Table 1. Numerical parameters used in the four regularization schemes. Λ_A is the regulator used in choice A, Λ_B the corresponding regulator of choice B, α_C and α_D are the regulators used in the choices C and D respectively. N is the number of bound states. For each set of data with the same regulator Λ_A, there is a corresponding figure that is indicated in the first column in the left. The scattering length is kept fixed at 5.4 fm in all cases, independent of the number of bound states.

Figure	N	V_0(MeV fm^2)	Λ_A(fm^{-1})	Λ_B(fm^{-1})	α_C(fm)	α_D(fm)
1	1	−0.6348	10	12.145	0.020 984	0.008 942
	2	−3.6000	10	8.830	0.131 200	0.044 080
	3	−14.030	10	6.488	0.403 600	0.112 400
	4	−40.132	10	5.200	0.870 300	0.211 380
2	1	−0.5306	20	25.420	0.008 515	0.003 693
	2	−2.2325	20	19.896	0.042 190	0.015 260
	3	−7.2221	20	15.395	0.119 400	0.036 880
	4	−17.705	20	12.838	0.238 200	0.065 960
3	1	−0.48935	30	38.930	0.005 158	0.002 261
	2	−1.80350	30	31.280	0.022 850	0.008 420
	3	−5.39250	30	24.785	0.062 700	0.020 185
	4	−12.4820	30	20.917	0.122 570	0.035 700

4. Numerical results and conclusions

In the following we present the results for phase-shifts, obtained by using four different regularization procedures of the previous section. The reduced mass m has been taken to be appropriate for the nucleon–nucleon system; $\hbar^2/(2m) = 41.47$ MeV fm^2. The range parameter μ of the potential has been taken to be 1 fm^{-1}. Although we have chosen nuclear units in our calculation, most aspects of this numerical study are of general interest.

In the renormalization scheme we define the cut-off parameter through one of the choices of regularization (for example, choice A), given by equation (23), and fix the scattering length to the experimental value ($a = 5.4$ fm, for the S-wave spin triplet nucleon–nucleon scattering) by adjusting the strength V_0 of the potential. The scattering length does not fix the number of bound states of the system and the strength of the potential fixes this number. In present renormalization we considered up to four bound states of the system. For other three regularization procedures (choices B, C and D) the strength V_0 and the corresponding number of bound states (obtained with choice A) are kept fixed together with the scattering length by redefining the corresponding cut-off parameters. With this procedure we guarantee that we are dealing with the renormalization of the same physical interaction via four regularization procedures. Presently, the physical observables that we fix by renormalization are the scattering length and the number of bound states. The numerical parameters used in calculation are given in table 1.

Although we consider up to four bound states of potential (1) and also consider the limit of very large momentum space cut-off, the situation of interest in the nucleon–nucleon system is the case of one bound state, the deuteron, and a finite cut-off determined by the 'size' of the problem. Hence, for the nucleon–nucleon system the first row in table 1 is of interest, where the momentum space cut-off is set at 10 fm^{-1}. We shall explore the off-shell behaviour of the nucleon–nucleon scattering under this situation.

In figures 1–3, we display four sets of curves for phase shift versus energy. In order to have compact figures, in all cases we set the zero-energy phase shift to π. Each set

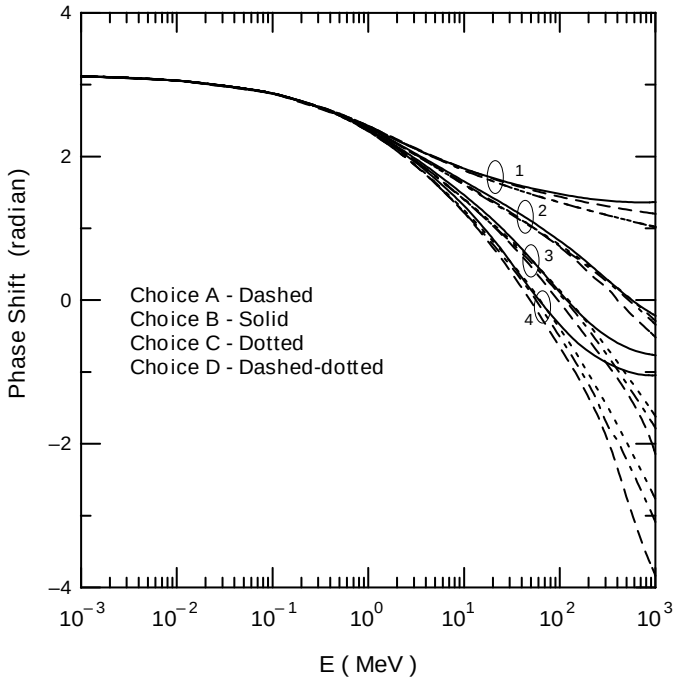

Figure 1. Renormalized phase shifts versus energy using four regularization procedures described in the text. The regulator used for choice A is $\Lambda_A = 10$ fm^{-1}. The corresponding regulators for the other three choices, and the corresponding strength V_0 that maintains the scattering length fixed at 5.4 fm, when varying the number of bound states N, are given in the first set of table 1.

is indicated by an ellipse and labelled by the number of bound states. In each set, there are four curves that represent four different regularization procedures. Schemes A–D are conveniently indicated inside the figures. The cut-off parameters of the four schemes are Λ_A, Λ_B, α_C, and α_D. In the renormalization limit the momentum cut-offs Λ_A and Λ_B should be large, and the configuration cut-offs α_C and α_D should be small. Also, the cut-offs should be large compared with the on-shell momentum. In schemes A–D this means $\Lambda_A^2 \gg k^2$, $\Lambda_B^2 \gg k^2$, $\alpha_C^{-2} \gg k^2$, and $\alpha_D^{-2} \gg k^2$, respectively.

By comparing the curves in each set of figure 1, we observe that the phase shifts are numerically very close for energies up to 50 MeV, that correspond to $k^2 \sim 1$ fm^{-2}, or $0.01\ \Lambda_A^2$. The deviations start to increase as energies approach the cut-off limit.

In figure 2, we repeat the same plots as in figure 1 with larger momentum cut-offs, Λ_A and Λ_B, or reduced configuration cut-offs, α_C and α_D. By increasing the momentum cut-off we approximate the renormalization limit of large cut-off. In this case, comparing the curves in each set, we observe that the phase shifts are numerically very close for energies up to 500 MeV, that correspond to $k^2 \sim 10$ fm$^{-2} \approx 0.025\ \Lambda_{\rm A}^2$.

The plots of figures 1 and 2 are repeated in figure 3 for a further increased momentum cut-off (reduced configuration cut-off). As we can see, the phase shifts, for each set of plots that have the same number of bound states, are very close to each other in all extension of the energies shown in the graph. The energies can go close to 1000 MeV, or $k^2 \sim 20$ fm$^{-2} \approx 0.025\ \Lambda_{\rm A}^2$.

As we can see from the three figures, the limit of validity of renormalization increases

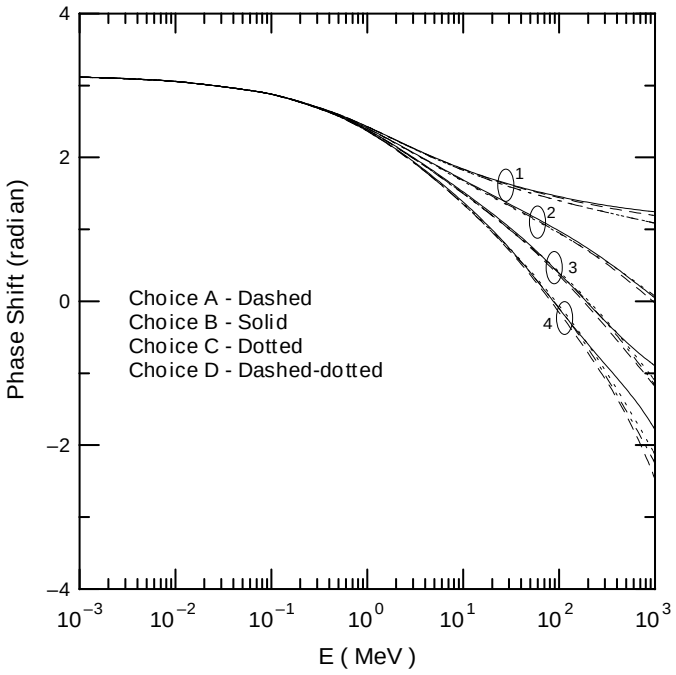

Figure 2. The same as in figure 1, using the parameters given in the second set of table 1, that have $\Lambda_A = 20$ fm^{-1}.

fast with the increase of the momentum cut-off. As expected, the renormalization becomes independent of different regularization procedures, if the momentum cut-off is large enough compared with the on-shell momentum or equivalently, the configuration cut-off is small enough. In this limit the domain of renormalization extends roughly up to 1 cm energy $E \approx 0.025\ E_\Lambda$ where $E_\Lambda = \hbar^2\Lambda^2/(2m)$.

For $k \ll \mu$, pure S-wave prevails and the scattering phase shift decreases linearly as k: $\delta \approx \pi - ka$. This behaviour is consistent with the phase shift of the contact interaction [5]: $\tan(\delta) = -ka$, which for small k reduces to $\delta \approx \pi - ka$. This is clearly represented in figures 1–3. This behaviour does not depend on the details of the potentials and on the number of bound states.

From table 1, and figures 1–3, it is interesting to observe that, even for $\mu \neq 0$, in the case of large cut-offs, the critical strength to produce four bound states is consistent with the limit given in equation (2). For the nucleon–nucleon system $V_{0,\mathrm{crit}} = -10.3675$ MeV fm^2. Note that in figure 3 we have a cut-off with 30 fm^{-1} and the corresponding $V_0(= -12.482$ MeV fm$^2)$. In the limit of very large cut-off and large number of bound states, V_0 should approach its critical value.

The cut-off behaviour of the renormalization scheme is shown in figure 4. In this figure we plot the dispersion in phase shifts among the four schemes A–D versus the cut-off parameter Λ_A in the case with four bound states. To show the dispersion in phase shifts we plot the differences between the phase shifts $\Delta\delta$ that show maximum deviation at a fixed energy: choices A and B. The three curves correspond to dispersion at three energies 150, 500, and 1000 MeV. As we can observe in this figure, the dispersion approaches zero as we go to the infinite momentum cut-off limit, and the results become independent of the

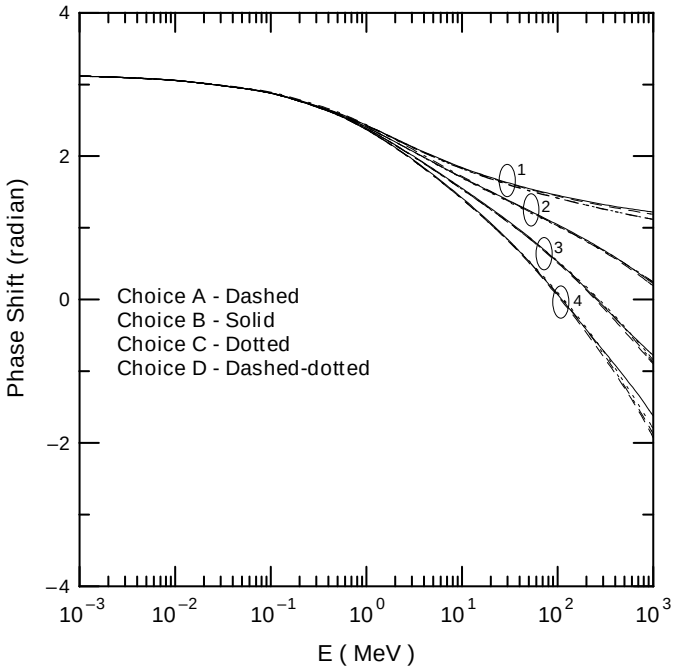

Figure 3. The same as in figure 1, using the parameters given in the third set of table 1, that have $\Lambda_A = 30$ fm^{-1}.

regularization procedure that have been used.

We have studied systems that can have up to four bound states, but as pointed out before, the situation of interest in the nucleon–nucleon system is the first row in table 1 where there is only one bound state and a finite momentum space cut-off of about 10 fm^{-1}. The situations with more than one bound states are of interest in atomic/molecular physics. Of the three momentum cut-offs used in this work the one at 10 fm^{-1} seems to be more appropriate for the nucleon–nucleon system.

The present work can be used to conclude the expected off-shell variation of different nucleon–nucleon potential models with the same physical content. Here we have used one constraint on the regularization scheme so as to fit the scattering length. In realistic situations several constraints are used in phenomenological nucleon–nucleon potentials so that the on-shell phase shifts of the different models are practically the same. However, t-matrices generated from such potentials may have large off-shell variations as pointed out in [12, 14]. As fully off-shell t-matrices are determined in terms of the half-shell t-matrices [12]. In figure 5 we plot the half-shell function (12) for the various schemes at following energies: $E_{\rm cm} = 0, 37.5, 140$, and 300 MeV. These were the energies explored by Fearing [14] in his study of Bremsstrahlung with different realistic potentials.

The half-shell variation in figure 5 is not a consequence of the on-shell variations observed in figures 1–3. At zero energy the four on-shell t-matrices are the same but they may have distinct off-shell behaviours. In the two cases (choices A and B) where momentum cut-offs were employed the regularization schemes are similar and there is no off-shell variation at low energies. The same is true for choices C and D. For the parameters used in the calculation we note that the momentum space cut-off functions (23) and (24) of choices A and B are quite different numerically. The same off-shell behaviour generated in these

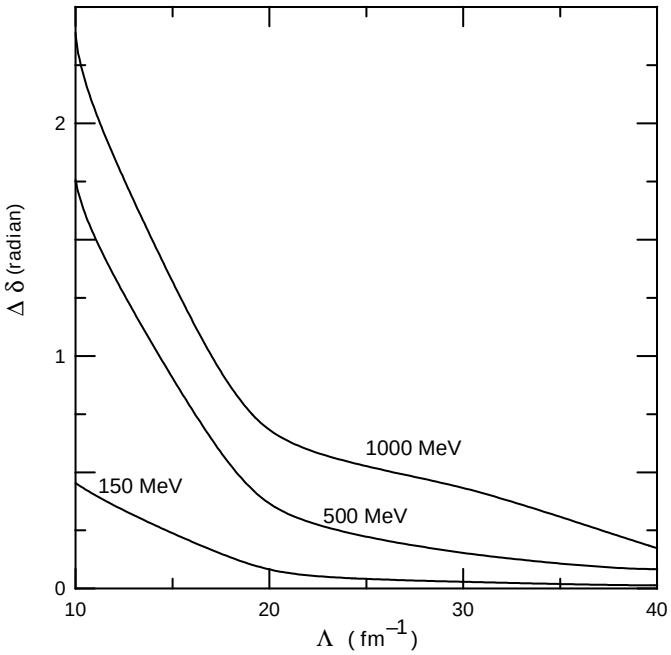

Figure 4. The dispersion in phase shifts $\Delta\delta$ versus the momentum cut-off Λ_A, for the energies 150, 500, and 1000 MeV, in the case we have four bound states. We define the dispersion by the difference between the phase shifts of choices A and B, which are enhanced for larger number of bound states N, as shown in figures 1–3

two choices suggests that such momentum space cut-offs in two phenomenological models should not lead to large off-shell variations independent of the values of the parameters used.

The off-shell variation of figure 5 is significantly lower than that observed by Fearing in different theoretical models. The larger half-shell variation he observed was possibly due to differences in the physical contents of the phenomenological nucleon–nucleon potential models. This indicates different intermediate-range (2–4 fm) behaviours of those realistic potentials. In the present study the long- and intermediate-range behaviours of the models are kept the same, while the short-range part of these potentials are varied in the different regularization schemes. This variation should increase as the momentum space cut-off Λ is reduced. For a fixed Λ it should increase as the momentum variables k or p of the half-shell function are increased. The present half-shell variations noted in figure 5 arise from the inherent differences in different regularization schemes. Similar half-shell variation(s) are expected in different phenomenological nucleon–nucleon potentials with same physical content.

In summary, we have tested numerically renormalization schemes using a singular local potential, that diverges at $r \to 0$ as the inverse of r^2. The scattering integral equation exhibits renormalizable ultraviolet divergences in this case. We performed numerical renormalizations with four regularization procedures, two with a cut-off in momentum space and two with a cut-off in configuration space. We find that the renormalization techniques are applicable to this case, such that, for lower energies compared with the cut-off, the results are independent of regularization procedures used to regularize the original equation. In

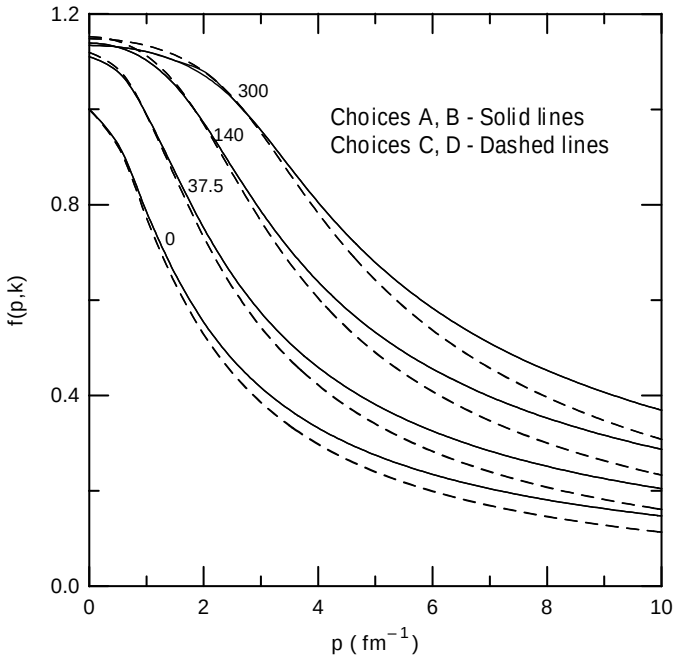

Figure 5. Off-shell function $f(p, k)$ versus p, for different regularization schemes corresponding to the first row of table 1. The curves are labelled by the respective centre-of-mass energies, in units of MeV.

the case of the nucleon–nucleon system the regularization scheme should maintain a single bound state and employ a finite cut-off. In that case we studied the off-shell variation of the different regularization schemes and found that the different phenomenological nucleon–nucleon potential models have larger off-shell variations [14] than found in the present study. Different intermediate-range behaviours of the usual phenomenological potentials are supposed to be responsible for larger off-shell variations. The present renormalization in the presence of up to four bound states is of relevance in atomic and molecular physics, and suggests that similar potentials in atomic and molecular physics can also be successfully renormalized in the present scheme.

Acknowledgments

We thank the Conselho Nacional de Desenvolvimento Científico e Tecnológico, Fundação de Amparo à Pesquisa do Estado de São Paulo, Coordenação de Aperfeiçoamento de Pessoal do Nível Superior and Financiadora de Estudos e Projetos of Brazil for partial financial support.

References

[1] Bjorken J D and Drell S D 1965 *Relativistic Quantum Fields* (New York: McGraw-Hill)
Feynman R P 1961 *Quantum Eletrodynamics* (New York: Benjamin)
Itzykson C and Zuber J B 1980 *Quantum Field Theory* (New York: McGraw-Hill)
Ryder L H 1985 *Quantum Field Theory* (Cambridge: Cambridge University Press)
Ramond P 1981 *Field Theory: A Modern Primer* (Reading, MA: Benjamin-Cummings)

[2] Wilson K G 1971 *Phys. Rev.* B **4** 3184
Wilson K G and Kogut J 1974 *Phys. Rep.* C **12** 78
[3] Manuel C and Tarrach R 1994 *Phys. Lett.* B **328** 113
[4] Gosdzinsky P and Tarrach R 1991 *Am. J. Phys.* **59** 70
Mead L R and Godines J 1991 *Am. J. Phys.* **59** 935
[5] Adhikari S K and Frederico T 1995 *Phys. Rev. Lett.* **74** 4572
[6] Weinberg S 1991 *Nucl. Phys.* B **363** 2
[7] Adhikari S K, Frederico T and Goldman I D 1995 *Phys. Rev. Lett.* **74** 487
[8] Beg M A B and Furlong R C 1985 *Phys. Rev.* D **31** 1370
[9] Landau L D and Lifchitz E M 1977 *Quantum Mechanics-Non Relativistic Theory* ch V (New York: Pergamon)
[10] Frank W M, Land K J and Spector R M 1971 *Rev. Mod. Phys.* **43** 1
[11] Amorim A E A, Tomio L and Frederico T 1992 *Phys. Rev.* C **46** 2224
[12] Redish E F 1987 *Nucl. Phys.* A **463** 417c
[13] Adhikari S K and Kowalski K L 1991 *Dynamical Collision Theory and its Applications* (New York: Academic)
[14] Fearing H W 1987 *Nucl. Phys.* A **463** 95c
[15] Jackiw R 1991 *M A B Beg Memorial Volume* eds A Ali and P Hoodbhoy (Singapore: World Scientific)
Gupta K S and Rajeev S G 1993 *Phys. Rev.* D **48** 5940
Case K M 1950 *Phys. Rev.* **80** 797
Parisi G and Zirilli F 1973 *J. Math. Phys.* **14** 243
[16] Marinari E and Parisi G 1991 *Europhys. Lett.* **15** 721
[17] Abramowitz M and Stegun I A (ed) 1968 *Handbook of Mathematical Functions* (New York: Dover)
[18] Tomio L and Adhikari S K 1980 *Phys. Rev.* C **22** 28
Tomio L and Adhikari S K 1980 *Phys. Rev.* C **22** 2359
[19] Tomio L and Adhikari S K 1995 *Chem. Phys. Lett.* **241** 477
[20] Gradshteyn I S and Ryzhik I M 1965 *Table of Integrals, Series, and Products* (New York: Academic)